Z. Phys. C - Particles and Fields 20, 207-212 (1983)

Zeitschrift für Physik C Particles and Fields

Inclusive γ and π^0 Production in e^+e^- Annihilation at 14, 22 and 34 GeV c.m. Energy

CELLO-Collaboration

H.J. Behrend, H. Fenner, M.-J. Schachter[1], V. Schröder, H. Sindt

Deutsches Elektronen-Synchrotron, DESY, D-2000 Hamburg, Federal Republic of Germany

G. D'Agostini, W.-D. Apel, J. Engler, G. Flügge, D.C. Fries, W. Fues, K. Gamerdinger, G. Hopp, H. Küster, H. Müller, H. Randoll, G. Schmidt[2], H. Schneider

Kernforschungszentrum Karlsruhe and Universität Karlsruhe, D-7500 Karlsruhe, Federal Republic of Germany

W. de Boer, G. Buschhorn, G. Grindhammer, P. Grosse-Wiesmann, B. Gunderson, C. Kiesling, R. Kotthaus, U. Kruse[3], H. Lierl, D. Lüers, H. Oberlack, P. Schacht

Max-Planck-Institut für Physik und Astrophysik, D-8000 München, Federal Republic of Germany

P. Colas, A. Cordier, M. Davier, D. Fournier, J.F. Grivaz, J. Haissinski, V. Journé, F. Laplanche, F. Le Diberder, U. Mallik, J.-J. Veillet

Laboratoire de l'Accélérateur Linéaire, F-91405 Orsay, France

J.H. Field[4], R. George, M. Goldberg, B. Grossetête, O. Hamon, F. Kapusta, F. Kovacs, G. London, L. Poggioli, M. Rivoal

Laboratoire de la Physique Nucléaire et Hautes Energies, University of Paris, F-75230 Paris, France

R. Aleksan, J. Bouchez, G. Carnesecchi, G. Cozzika, Y. Ducros, A. Gaidot, Y. Lavagne, J. Pamela, J.P. Pansart, F. Pierre

Centre d'Etudes Nucléaires, Saclay, F-9110 Gif-sur-Yvette, France

Received 5 August 1983

Abstract. We have measured the scale invariant inclusive photon and π^0 cross sections at $W=14$, 22 and 34 GeV. A comparison with $\pi^\pm$ data shows no significant difference between neutral and charged pion production. Comparing the integrated cross sections in the x range $0.15<x<1.0$ we observe a considerable decrease from 14 GeV to 34 GeV with a statistical significance of 1.5 standard deviations. This is compatible with the expectations for scaling violations from QCD.

I. Introduction

In the quark-parton model the e^+e^- annihilation into hadrons is expected to proceed via the pair production of quarks. The subsequent fragmentation into hadrons is predicted to depend only on $x = 2E/W$ with E being the particle energy and W the c.m. energy. This scale invariance is broken in QCD because of gluon bremsstrahlung. In the PETRA energy range non-perturbative mass effects are still important and may contribute substantially even in the large x region [1]. Significant scale breaking has been observed in inclusive charged hadron production [2, 3]. In addition, some indications for scale breaking have been found in inclusive π^0 and $\pi^\pm$ production [4, 5]. This paper presents an analysis of

[1] Now at SCS, Hamburg, FRG
[2] Now at DESY, Hamburg, FRG
[3] Now at University of Illinois, Urbana, USA
[4] On leave of absence from DESY, Hamburg, FRG

the energy dependence of the inclusive π^0 production with a special emphasis on the large x region. We extend the previous analysis [6] using data at $W=14$, 22 and 34 GeV.

II. Detector and Data Selection

The data were taken with the CELLO detector [7] at PETRA at average c.m. energies of $W=14$, 22 and 34 GeV. The corresponding integrated luminosities are 1.3 pb^{-1}, 2.5 pb^{-1}, 7.9 pb^{-1}.

Charged particles were measured in cylindrical drift and proportional chambers in a $1.3\,T$ magnetic field yielding a momentum resolution of $\sigma(p)/p=2\% \cdot p \cdot \sin\theta$ (p *in* GeV) over 92% of the solid angle. For neutral particle reconstruction we use the barrel part of a fine grain lead liquid argon calorimeter which has a solid angle acceptance of 86% of 4π. Each of 16 calorimeter modules samples the energy deposited by particles in the liquid argon 17 times in depth. The energy is collected on lead strips of three different orientations up to a maximum of 21 radiation lengths (X_0). For each particle this information is combined into six energy clusters in depth. The trajectory and energy of the particle are thus reconstructed from up to six energy and position measurements. We obtain an energy resolution of $\sigma(E)/E=13\%/\sqrt{E}$ (E in GeV) and an angular resolution of 4 mrad. The jet structure of the multihadronic final states causes a substantial overlap between clusters of deposited charge from different photons as well as photons and charged tracks. Thus, depending on the event topology and the photon energies involved, the energy resolution may be deteriorated by as much as a factor of two.

The trigger for the multihadronic final state and the event selection criteria have been described previously [8]. The most relevant data selection requirements were:

a) more than 4 reconstructed charged particles,
b) fraction of total "visible energy" in charged particles

$$\sum E_i/W > 0.24.$$

Theses cuts remove two-photon events very efficiently. The residual background (2.7%) from cosmic rays, beam-gas- and Bhabha-events has been removed by visual scan. The corresponding numbers of multihadronic events are then 2303, 1772 and 2590 respectively at the three energies.

III. Inclusive Photons

The data were processed through the reconstruction programs for charged particle tracks in the inner detector and for showers in the barrel liquid argon calorimeter ($|\cos\theta|<0.86$).

In the shower reconstruction program clusters in each of the six layers of the modules are reconstructed using the geometrical correlations between the three channel orientations and between neighbouring channels in depth. Thus up to six two-dimensional clusters are formed and then linked to give the full three-dimensional showers. A topology determination – single or several overlapping photons – is done by scanning the two-dimensional clusters for structures in the pulse height distribution and testing their spatial distribution. Monte-Carlo (MC) studies show that the efficiency and resolution for two photons separated by an angle larger than 130 mrad are similar to those for single photons. At an angle of 65 mrad the efficiency for separating two photons is still about 50%. The energy and angular resolutions are, in this case, worse by up to a factor of two depending on the photon energies considered.

Tracks found in the inner detector are extrapolated into the liquid argon calorimeter and the extrapolated track position is used in the two-dimensional cluster reconstruction. Thus the final showers are separated into "charged showers" (showers which are found to be linked to charged tracks) and "neutral showers" (showers for which no link is found to charged tracks). The efficiency of this linking procedure for tracks with momenta above 1 GeV was found to be 74% in multihadronic events. The longitudinal development of the neutral showers is then used to distinguish photons from K^0's, neutrons or charged particles where the link failed. For the selection of well measured photons the following criteria are used:

– Photons that result from three or more overlapping showers are rejected.
– Neutral showers are only accepted if more than 20% of the total charge is deposited in the second and third layer of the liquid argon calorimeter extending from 3 to $8\,X_0$.
– Showers corresponding to an energy of less than 3 GeV are only accepted if no charge is found in the sixth layer ($>16\,X_0$).
– Photons whose showers overlap with clusters linked to charged tracks are rejected.
– Two photons with overlapping showers are kept only if the double structure found in the reconstruction program is present in the second and third layer, which are the layers that have a fine lateral sampling.
– Photons whose showers do not extend in depth over at least three layers are rejected.
– The minimum photon energy is 300 MeV.

These cuts were checked using Bhabha events and M.C. generated multihadronic events. The resulting efficiency due to these shower cuts for reconstructed photons for energies above 300 MeV is 27% at $W=34$ GeV. The background due to misidentified n or K_L^0, or due to charged particles where the link failed is less than 1.0% as obtained from MC studies.

Corrections for acceptance, reconstruction inefficiencies, losses due to all cuts described above and for radiative effects were determined by MC methods. Multihadron events were generated assuming $q\bar{q}$ and $q\bar{q}g$ production according to first order QCD (Hoyer et al., [9]) with subsequent fragmentation (Field-Feynman, [10]).*

These events were processed through a detailed detector simulation using the EGS and HETC codes [11] for the simulation of charge deposition in the liquid argon calorimeter and through the same reconstruction chain as the real data.

Figure 1 shows the scale invariant differential cross section $s\frac{d\sigma}{dx}$ for inclusive photon production at $W=14$, 22 and 34 GeV together with the corresponding cross sections from LGW at SPEAR [12] at lower energies. The error bars indicate the statistical errors and all systematic errors due to absolute normalization (5% at $W=22$ and 34 GeV and 10% at $W=14$ GeV), calibration (6%) and MC simulation (10%), added in quadrature. The data at the three c.m. energies do not show any prominent structures and are lower than the corresponding cross sections from LGW. Only part of the difference may be explained by the systematic error of approximately

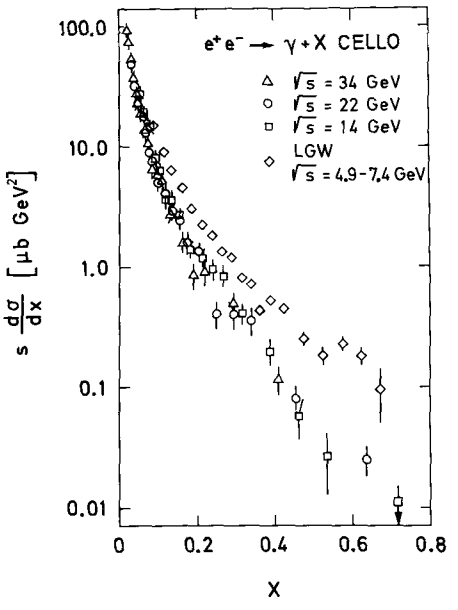

Fig. 1. Cross sections $s\frac{d\sigma}{dx}$ for inclusive photon production at $W=14$, 22 and 34 GeV in comparison to data from SPEAR [12]

20% for the LGW data due to the absolute normalisation (not shown in Fig. 1). Whereas the data at $W=22$ GeV and $W=34$ GeV are within the errors compatible with scale invariance, the data at $W=14$ GeV yield somewhat larger cross sections.

IV. π^0-Production

a) π^0 Cross Sections for Momenta
$0.9<p_{\pi^0}<8.0$ GeV/c (Methods A)

To study π^0 production, all invariant mass combinations $m_{\gamma\gamma}$ of two photons in a given event are constructed. Figure 2 shows the distribution of these masses for the three c.m. energies. A fit to the data using a gaussian plus a background term, given by a

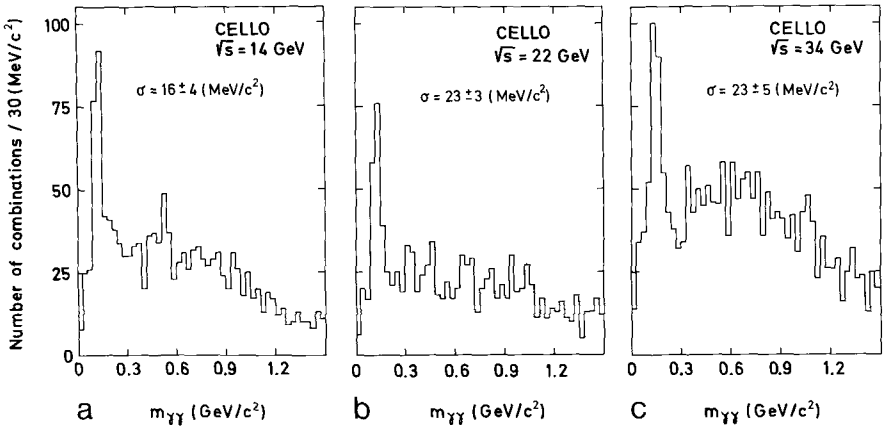

Fig. 2a–c. Distribution of the invariant mass combinations of all photon pairs at $W=14$, 22 and 34 GeV

* Parameters used at $W=34$ GeV: The mean transverse momentum for quarks and gluons $\sigma=0.30$ GeV/c, the relative abundance of u,d,s quarks from the sea 3:3:1, the relative proportion of pseudoscalar and vector mesons produced $P/(P+V)=0.55$, the fragmentation parameter in the Feynman-Field parameterization $AF=0.70$, the strong coupling constant $\alpha_s=0.19$

second order polynomial, yields a width of the π^0 peak of $\sigma = 16 \pm 4$, 23 ± 3 and 23 ± 5 (MeV/c^2) at $W = 14$, 22 and 34 GeV respectively.

For the determination of the inclusive π^0 cross section, two different methods were applied. In the first method (A1) the χ^2 corresponding to the π^0 hypothesis was calculated for $m_{\gamma\gamma}$ from all two photon combinations. First the two photons with the lowest χ^2 were selected, then from the remaining photons the two with the lowest χ^2 were found. This procedure has been repeated until χ^2 was unacceptably large. For the photons thus selected a regrouping into all possible pair combinations was tried through all permutations, and the permutation yielding the lowest sum of all individual χ^2 contributions was kept. Finally a π^0 candidate was kept only if $m_{\gamma\gamma}$ was in the range $60 < m_{\gamma\gamma} < 210$ MeV/c^2. Depending on the π^0-momentum, this yields an overall acceptance increasing from 5.3% ($E_{\pi^0} = 3.5$ GeV) at $W = 34$ GeV to 12.6% ($E_{\pi^0} = 3.5$ GeV) at $W = 14$ GeV. The background due to wrong $\gamma\gamma$-combinations, as determined from MC, varies with the c.m. energy being highest at $W = 34$ GeV where it is 14% in average for π^0 momenta above 1.2 GeV/c, and substantially larger (37%) for momenta below 1.2 GeV/c.

In the second method (A2), the π^0 cross section has been obtained using a simple background subtraction. All possible combinations of γ-pairs were binned according to the momentum of the pair. For each momentum bin the background was estimated by forming pairs with γ's coming from different events. The correlation of the photons due to the jet structure was taken into account by rotating each event so that the sphericity axes coincide. The background for each π^0 momentum bin thus determined was normalized using the mass spectrum above the π^0 mass ($270 < m_{\gamma\gamma} < 450$ MeV/c^2). The π^0 mass interval was $60 < m_{\gamma\gamma} < 210$ MeV/c^2. The π^0 cross sections from the two methods were in good agreement and therefore the average of both methods was used.

The various contributions to the systematic error due to MC simulation (20%), calibration (6%) and absolute normalization (5% at $W = 22$ and 34 GeV and 10% at $W = 14$ GeV) have been added in quadrature.

b) π^0 Cross Sections for Momenta $p_{\pi^0} > 4$ GeV/c (Method B)

The efficiency to reconstruct high energy π^0's from the two decay photons depends strongly on the probability to resolve two nearby photons in the liquid argon calorimeter. Given the granularity of the liquid argon calorimeter, this reconstruction efficiency decreases rapidly in the momentum interval $6.0 < P_{\pi^0} < 8.0$ GeV/c. For higher π^0 momenta only one single neutral shower is detected in the calorimeter. We therefore determined the π^0 cross sections from single, high energetic neutral showers.

With MC generated events we obtain an acceptance matrix A_{ij} by determining the probability for a π^0 from an energy bin E_i to be reconstructed as a single neutral shower into an energy bin E_j within a cone of 5 degrees around the original π^0 direction of flight. To select preferentially well measured showers resulting from photons, we used very similar cuts to those applied for the selection of photons described in Chap. 2. The modified criteria are:

– We accept neutral showers if the charge deposited in the second and third layer exceeds 10% (instead of 20%) of the total charge.
– To increase the efficiency for high energy photons and π^0's we do not reject charged showers if the energy is more than twice the measured momentum and the momentum is below 2 GeV/c. Thus we recover part of those high energy neutral showers that accidentally overlap with a charged particle track to a level where the reconstruction program is unable to resolve the two showers.

Based on this acceptance matrix we then calculate the π^0 cross sections from the yield of single neutral showers in the data. This determination depends on our ability to describe all relevant sources of photons in our MC. We have tested the procedure by applying this method to high energy bremsstrahlung photons. We obtained good agreement between the measured and predicted yield. This verifies the assumption made in the MC that the majority of high energy photons are either bremsstrahlung photons or the decay products of high energy π^0's and η's. No other strong source of photons is observed.

The systematic errors are quite similar to those quoted in Chap. IVa, except for the systematic error due to the calibration. Taking the x-dependence of this error into account and adding all systematic errors in quadrature, we obtain total systematic errors of 20% to 30%.

c) Results

The resulting scale invariant cross sections $\frac{s}{\beta}\frac{d\sigma}{dx}$ for inclusive π^0-production (see Table 1) as obtained from the two methods described in Chap. IVa (open symbols) and IVb (full symbols) are compared in Fig. 3 with the $\pi^\pm$ cross sections from TASSO [5]. The errors include the statistical and systematic ones

Table 1. The differential cross section $\frac{s}{\beta}\frac{d\sigma}{dx}$ for $e^+e^- \to \pi^0 X$. The errors include all statistical and systematic errors

$W=14$ GeV		$W=22$ GeV		$W=34$ GeV	
$\langle x \rangle$	$\frac{s}{\beta}\frac{d\sigma}{dx}$ [μb GeV^2]	$\langle x \rangle$	$\frac{s}{\beta}\frac{d\sigma}{dx}$ [μb GeV^2]	$\langle x \rangle$	$\frac{s}{\beta}\frac{d\sigma}{dx}$ [μb GeV^2]
Method A					
0.148	4.60 ±1.21	0.094	8.15 ±1.87	0.061	14.85 ±4.31
0.207	1.95 ±0.50	0.133	3.07 ±0.66	0.086	9.10 ±1.98
0.294	0.84 ±0.23	0.188	1.81 ±0.43	0.122	4.62 ±1.10
0.381	0.34 ±0.11	0.243	0.92 ±0.25	0.158	2.08 ±0.63
0.487	0.13 ±0.05	0.313	0.36 ±0.11	0.203	1.18 ±0.34
0.667	0.006 ±0.006	0.435	0.14 ±0.05	0.284	0.52 ±0.18
		0.619	0.016 ±0.016	0.402	0.17 ±0.17
Method B					
0.667	0.0129 ±0.0070	0.435	0.176 ±0.046	0.284	0.581 ±0.134
0.915	0.0 ±0.004	0.619	0.050 ±0.017	0.402	0.194 ±0.053
		0.847	0.0076 ±0.0046	0.580	0.059 ±0.017
				0.840	0.0126 ±0.0057

added in quadrature. In the x range of overlap the results of both methods give good agreement for all three c.m. energies. The results for small x at $W=34$ GeV are somewhat lower in comparison to our previous analysis [6]. This is attributed to an increase in acceptance at low x due to a more detailed MC simulation of the detector reducing thus the corrections, the raw data remaining unchanged. At the three c.m. energies we find good agreement between the π^0 and $1/2(\pi^+ + \pi^-)$-cross sections. For a more detailed comparison an exponential Ae^{-Bx} was fitted to the data in the region $x > 0.15$. The integrals over the range $0.2 < x < 0.6$ were computed. These integrated cross sections are compared in Table 2a with the corresponding result for $1/2 \cdot (\pi^+ + \pi^-)$ from TASSO [5]. For the ratio $2\pi^0/(\pi^+ + \pi^-)$ we thus obtain 1.21 ± 0.42, 0.96 ± 0.40 and 1.01 ± 0.35 at $W = 14$, 22 and 34 GeV respectively. Neutral pions behave like charged pions.

Comparing our π^0-cross sections with those from TASSO [4], we find good agreement at $W=34$ GeV in the x-range of overlap $x < 0.2$. In contrast, our

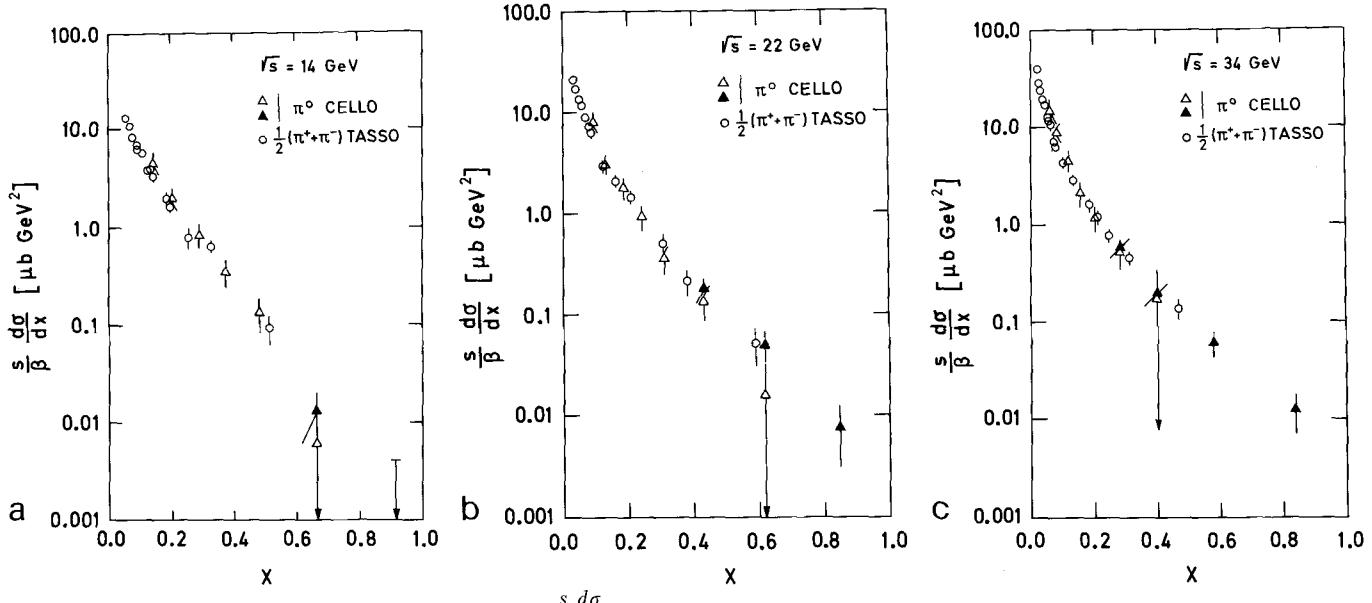

Fig. 3a–c. Comparison of the inclusive cross sections $\frac{s}{\beta}\frac{d\sigma}{dx}$ for π^0 production at $W=14$, 22 and 34 GeV with one half of the inclusive charged pion cross section [5]

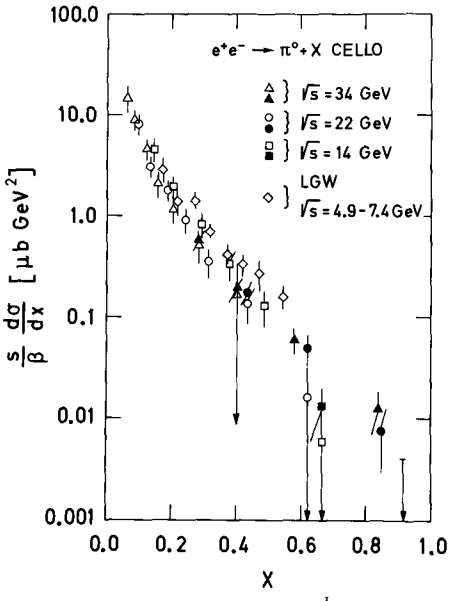

Fig. 4. Inclusive cross sections $\frac{s}{\beta}\frac{d\sigma}{dx}$ for π^0 production at $W=14$, 22 and 34 GeV. In addition π^0 inclusive data from lower energies [12] are also shown

Table 2a. Integrated inclusive cross section $\sigma = \int_{0.2}^{0.6} \frac{s}{\beta}\frac{d\sigma}{dx}$ for π^0 and $1/2\,(\pi^+ + \pi^-)$ [5]

W [GeV]	$\sigma\,(\pi^0)$ [μb GeV^2]	$\sigma(1/2(\pi^+ + \pi^-))$ [μb GeV^2]	$\frac{2\pi^0}{\pi^+ + \pi^-}$
14	0.204 ± 0.066	0.168 ± 0.021	1.21 ± 0.42
22	0.140 ± 0.055	0.146 ± 0.019	0.96 ± 0.40
34	0.137 ± 0.045	0.135 ± 0.016	1.01 ± 0.35

Table 2b. Integrated inclusive cross section $\sigma = \int_{0.15}^{1.0} \frac{s}{\beta}\frac{d\sigma}{dx}$ for π^0 from LGW [12] and CELLO

W [GeV]	σ [b GeV^2]
5.9–7.4[a]	0.391 ± 0.126
14	0.364 ± 0.118
22	0.224 ± 0.087
34	0.212 ± 0.070

[a] Using the data from [12] we have determined the integrated cross section using a fit $A \cdot e^{-Bx}$

data at $W=14$ GeV are considerably higher than, but still compatible with those from [4].

In Fig. 4 we compare our π^0 cross sections for the three c.m. energies with those from SPEAR [12] at lower energies. Whereas the data at $W=14$ GeV show agreement with those from LGW, the cross sections at $W=22$ and 34 GeV are considerably lower. Between $W=22$ GeV and $W=34$ GeV the scale invariant cross sections do not indicate a significant energy variation. A more detailed comparison is obtained from the integrated cross sections in the x-region $0.15 < x < 1.0$ (see Table 2b): While the values of the integrated cross sections do not change between $W=5.9$–7.4 GeV and $W=14$ GeV, they decrease considerably with a statistical significance of 1.5 standard deviations between $W=14$ GeV and $W=34$ GeV.

If we vary the fragmentation parameters in the MC models within reasonable limits, the predicted π^0-yields change by as much as the error in our measurement. Thus non-perturbative mass effects may be of similar size as QCD-expectations for scaling violation due to gluon-bremsstrahlung. Such effects cannot be separated at present PETRA energies. Our results are compatible with these expectations.

Acknowledgement. We are indebted to the PETRA machine group and the DESY computer center for their excellent support during the experiments. We acknowledge the invaluable effort of all engineers and technicians of the collaborating institutions in the construction and maintenance of the apparatus, in particular the operation of the magnet system by G. Mayaux and Dr. Horlitz and their groups. The visiting groups wish to thank the DESY directorate for the support and kind hospitality extended to them. This work was partly supported by the Bundesministerium für Forschung und Technologie.

References

1. C. Peterson et al.: Phys. Rev. **D27**, 105 (1983)
2. TASSO-Collab. R. Brandelik et al.: Phys. Lett. **114B**, 66 (1982)
3. MARK II-Collab. J.F. Patrick et al.: Phys. Rev. Lett. **49**, 1232 (1982)
4. TASSO-Collab. R. Brandelik et al.: Phys. Lett. **108B**, 71 (1982)
5. TASSO-Collab. R. Brandelik et al.: Phys. Lett. **113B**, 98 (1982)
6. CELLO-Collab. H.J. Behrend et al.: Z. Phys. C – Particles and Fields **14**, 189 (1982)
7. CELLO-Collab. H.J. Behrend et al.: Phys. Scr. **23**, 610 (1981)
8. CELLO-Collab. H.J. Behrend et al.: DESY 81-029 (1981)
9. P. Hoyer et al.: Nucl. Phys. **B161**, 349 (1979)
10. R.D. Field, R.P. Feynman: Phys. Rev. **D15**, 2590 (1977); Nucl. Phys. **B136**, 1 (1978)
11. R.L. Ford, W.R. Nelson: EGS Code, SLAC-Report 210 (1978); RSIC Computer Code Collection, HETC Code, Oak Ridge National Laboratory, CCC-178
12. MARK I-LGW-Collab. D.L. Scharre et al.: Phys. Rev. Lett. **41**, 1005 (1978)